Neurobiology of Disease 69 (2014) 225–234

Contents lists available at ScienceDirect

Neurobiology of Disease

journal homepage: www.elsevier.com/locate/ynbdi

Mechanism underlying unaltered cortical inhibitory synaptic transmission in contrast with enhanced excitatory transmission in $Ca_V2.1$ knockin migraine mice

Dania Vecchia [a], Angelita Tottene [a], Arn M.J.M. van den Maagdenberg [b], Daniela Pietrobon [a,*]

[a] Department of Biomedical Sciences, University of Padova and CNR Institute of Neuroscience, 35121 Padova, Italy
[b] Department of Human Genetics and Neurology, Leiden University Medical Centre, Leiden, The Netherlands

ARTICLE INFO

Article history:
Received 29 January 2014
Revised 7 May 2014
Accepted 27 May 2014
Available online 5 June 2014

Keywords:
Migraine, calcium channel, inhibitory synaptic transmission
Fast-spiking interneuron
Knockin mouse model
Channelopathy
Excitatory–inhibitory balance

ABSTRACT

Familial hemiplegic migraine type 1 (FHM1), a monogenic subtype of migraine with aura, is caused by gain-of-function mutations in $Ca_V2.1$ (P/Q-type) calcium channels. In FHM1 knockin mice, excitatory neurotransmission at cortical pyramidal cell synapses is enhanced, but inhibitory neurotransmission at connected pairs of fast-spiking (FS) interneurons and pyramidal cells is unaltered, despite being initiated by $Ca_V2.1$ channels. The mechanism underlying the unaltered GABA release at cortical FS interneuron synapses remains unknown. Here, we show that the FHM1 R192Q mutation does not affect inhibitory transmission at autapses of cortical FS and other types of multipolar interneurons in microculture from R192Q knockin mice, and investigate the underlying mechanism. Lowering the extracellular $[Ca^{2+}]$ did not reveal gain-of-function of evoked transmission neither in control nor after prolongation of the action potential (AP) with tetraethylammonium, indicating unaltered AP-evoked presynaptic calcium influx at inhibitory autapses in FHM1 KI mice. Neither saturation of the presynaptic calcium sensor nor short duration of the AP can explain the unaltered inhibitory transmission in the mutant mice. Recordings of the P/Q-type calcium current in multipolar interneurons in microculture revealed that the current density and the gating properties of the $Ca_V2.1$ channels expressed in these interneurons are barely affected by the FHM1 mutation, in contrast with the enhanced current density and left-shifted activation gating of mutant $Ca_V2.1$ channels in cortical pyramidal cells. Our findings suggest that expression of specific $Ca_V2.1$ channels differentially sensitive to modulation by FHM1 mutations in inhibitory and excitatory cortical neurons underlies the gain-of-function of excitatory but unaltered inhibitory synaptic transmission and the likely consequent dysregulation of the cortical excitatory–inhibitory balance in FHM1.

Introduction

Voltage-gated P/Q-type calcium channels ($Ca_V2.1$) play a prominent role in controlling neurotransmitter release at brain excitatory and inhibitory synapses (Pietrobon, 2005, 2010). Mutations in the gene encoding the $Ca_V2.1\alpha1$ subunit cause several neurological disorders including familial hemiplegic migraine type 1 (FHM1), a rare monogenic form of migraine with aura (Ophoff et al., 1996; Pietrobon, 2010). Migraine is a common disabling disorder caused by a primary brain dysfunction that leads to episodic activation of the trigeminovascular pain pathway and headache (Pietrobon and Moskowitz, 2013). There is increasing evidence that the headache mechanisms can be triggered by cortical spreading depression (CSD), the phenomenon underlying migraine aura (Pietrobon and Moskowitz, 2013). The molecular and cellular mechanisms of the primary brain dysfunction(s) leading to susceptibility to CSD and to the migraine attack remain a major open issue. Important insights into these mechanisms have been obtained from the analysis of functional consequences of FHM1 mutations, revealing that these mutations produce: (i) gain-of-function of human recombinant and native neuronal mouse $Ca_V2.1$ channels, mainly due to channel activation to lower voltages and increased channel open probability; and (ii) facilitation of induction and propagation of experimental CSD, due to increased glutamate release at cortical pyramidal cell synapses [(Pietrobon, 2010; Pietrobon and Moskowitz, 2013) and references therein]. In

Abbreviations: AHP, after-hyperpolarization; AP, action potential; AP_{hw}, action potential half width; BME, basal Eagle's medium; BSA, bovine serum albumin; CGRP, calcitonin gene-related peptide; CSD, cortical spreading depression; DIV, days in vitro; FHM1, familial hemiplegic migraine type 1; FS, fast-spiking; GABA, gamma-aminobutyric acid; GAD, glutamic acid decarboxylase; 5HT3aR, 5-hydroxytryptamine 3a receptor; KI, knockin; LJP, liquid junction potential; PBS, phosphate buffered saline; PV, parvalbumin; siRNA, small interfering ribonucleic acid; SNAP25, synaptosomal-associated protein of 25 kDa; SOM, somatostatin; VIP, vasoactive intestinal peptide.

* Corresponding author at: Dept. of Biomedical Sciences, University of Padova, V.le G. Colombo 3, 35121 Padova, Italy.
E-mail address: daniela.pietrobon@unipd.it (D. Pietrobon).
Available online on ScienceDirect (www.sciencedirect.com).

http://dx.doi.org/10.1016/j.nbd.2014.05.035

striking contrast with enhanced glutamatergic neurotransmission, the inhibitory neurotransmission at connected pairs of layer 2/3 fast-spiking (FS) interneurons and pyramidal cells was unaltered in FHM1 knockin (KI) mice, despite being initiated by $Ca_V2.1$ channels (Tottene et al., 2009). The differential effect of FHM1 mutations at excitatory and inhibitory synapses suggests altered regulation of the cortical excitatory–inhibitory balance in FHM1 and supports the view of migraine as a disorder of brain excitatory–inhibitory balance (Pietrobon and Moskowitz, 2013; Vecchia and Pietrobon, 2012).

The lack of effect of FHM1 mutations on GABA release at FS interneuron synapses is puzzling and the underlying mechanism remains unknown. Several possible mechanisms were suggested, including: (i) saturation of the presynaptic calcium sensor; (ii) short duration of the action potential (AP) leading to unaltered AP-evoked presynaptic Ca^{2+} (Ca) influx despite shifted activation of mutant $Ca_V2.1$ channels to lower voltages; and (iii) interneuron-specific $Ca_V2.1$ channels whose gating properties are not affected by the FHM1 mutation (Fioretti et al., 2011; Inchauspe et al., 2010; Tottene et al., 2009; Xue and Rosenmund, 2009). Another interesting question is whether other inhibitory synapses, besides the FS interneuron-pyramidal cell synapse, are unaffected by FHM1 mutations.

Here, we show that the FHM1 R192Q mutation does not affect inhibitory transmission at autapses of cortical FS and other types of multipolar interneurons in microculture, and we investigate the mechanisms underlying this lack of effect despite a dominant role of P/Q channels in controlling GABA release. Our findings support the conclusion that the unaltered inhibitory transmission at multipolar (mainly FS) interneuron autapses is due to the expression of specific $Ca_V2.1$ channels whose gating is barely affected by the FHM1 mutation, and not to near saturation of the presynaptic calcium sensor or short duration of the AP.

Materials and methods

Preparation of cortical neurons in microculture

Cortical neurons were isolated from P0-2 homozygous KI mice carrying the $Ca_V2.1$ FHM1 R192Q mutation (van den Maagdenberg et al., 2004) and wild-type (WT) C57Bl6J mice with the same genetic background following the procedure of Levi et al. (1984). The neurons were cultured on glial microislands (at the density of 6000–25,000 cells/ml) essentially as reported in Brody and Yue (2000) for hippocampal neurons, except for the following details: astrocytes culture medium was basal Eagle's medium (BME) plus 10% fetal bovine serum, 25 mM KCl, 2 mM glutamine and 50 μg/ml gentamicin; neuronal medium was Neurobasal A plus 2% B27 Supplement, 0.5 mM glutamine and 1% PSN Antibiotic mix (all from Gibco); only half volume of astrocytes medium was replaced with neuronal medium to allow the astrocytes to condition the medium before neuron plating. Every 4 days half volume of neuronal medium was changed with a fresh one.

Single cortical neurons grown on glial microislands form synaptic connections onto themselves (autapses). These autaptic connections are by definition monosynaptic, offer an unusually homogeneous population of synapses producing large synaptic responses and solution exchanges can be fast and complete (Bekkers and Stevens, 1991).

All experimental procedures were carried out in accordance with the Italian Animal Welfare Act and with the Use Committee guidelines of the University of Padova and were approved by the local authority veterinary service.

Immunofluorescence assays

Cells grown on glial microislands for 12 days were washed with phosphate buffered saline (PBS), fixed for 20 minutes at room temperature with 4% paraformaldehyde, 4% sucrose in PBS, quenched (0.38% glycine, 0.24% NH_4Cl in PBS, twice for 10 minutes each) and permeabilized with 5% acetic acid in ethanol for 20 minutes at −20 °C. After saturation with 3% bovine serum albumin (BSA) and 10% goat serum in PBS for 20 minutes, samples were incubated with the primary antibodies (diluted in 3% BSA, 10 % goat serum in PBS) for 60 minutes at room temperature. Mouse monoclonal anti-glutamic acid decarboxylase (GAD-67; from Millipore, Billerica, MA, USA) was used at dilution of 1:500; rabbit polyclonal anti-parvalbumin (PV; from Abcam, Cambridge, UK) was used at dilution of 1:300; rat monoclonal anti-somatostatin (SOM; from Millipore) was used at a dilution of 1:100. The specific primary antibodies were detected with Alexa-conjugated secondary antibodies raised in goat (anti-mouse 488, anti-rabbit 647, anti-rat 568; from Life Technologies, Monza, Italy), which were incubated for 60 minutes at room temperature after washing with 3% BSA in PBS; working dilution 1:200 in 3% BSA, 10% goat serum. Coverslips were mounted in mowiol (Sigma). Images were acquired with a DMI6000 inverted epifluorescence microscope (Leica, Germany) equipped with a HCX PL APO 60× oil immersion objective NA 1.4. Differential interference contrast microscopy was used to increase contrast for brightfield imaging of the cultures. Images were acquired with an Orca-Flash4 digital camera (Hamamatsu, Japan).

Electrophysiological recordings and data analysis

Whole-cell patch-clamp recordings were made at room temperature following standard techniques. Electrical signals were recorded through an Axopatch-200B patch-clamp amplifier and digitized using a Digidata 1440A interface and pClamp software (Axon Instruments). Compensation (typically 60–80%) for series resistance was used (5–6 MΩ after compensation).

Microislands containing several glial cells and a single neuron with irregular soma morphology and multiple asymmetrical processes emanating from it (multipolar interneuron; Fig. 1) were selected for recording of evoked postsynaptic currents (PSCs) in voltage-clamp mode (sampling 5 KHz; filter 1 KHz) after 10 to 14 days (DIVs) in culture. Given the well known large diversity of cortical interneurons (Petilla Interneuron Nomenclature Group, 2008; Rudy et al., 2011), to limit the heterogeneity, cells characterized by fusiform ovoid or spindle-shaped soma with symmetrical processes (Fig. 1) were not considered (to exclude bitufted and bipolar interneurons). Immunofluorescence using antibodies specific for PV and/or SOM revealed that almost all PV-expressing (PV+) interneurons had morphology similar to that of the cells selected for recordings (multipolar interneurons: Fig. 1C) whereas 61% of SOM-expressing (SOM+) interneurons had fusiform ovoid or spindle-shaped soma; the remaining 39% had multipolar morphology similar to that of some of the cells selected for recordings (Fig. 1D).

APs in the unclamped processes were induced by a 2 ms voltage pulse to +20 mV every 10 s from a holding potential of −80 mV. The evoked PSCs were measured at −90 mV.

The pipette solution contained (in mM): 110 K-methanesulfonate, 5 $MgCl_2$, 30 HEPES, 3 EGTA, 4 ATP, 0.5 GTP and 1 cAMP (pH 7.4 with KOH). The extracellular solution contained (in mM): 145 NaCl, 3 KCl, 10 HEPES, 10 glucose, 1 $MgCl_2$, 2 $CaCl_2$ (pH 7.4 with NaOH). In the experiments testing the effect of the peptide toxin ω-AgaIVA (Peptide Institute Inc.), cytochrome C (0.1 mg/ml) was added to the solution.

Although the $GABA_A$-mediated inhibitory postsynaptic currents (IPSCs) recorded at −90 mV are inward currents (given the predicted and measured E_{rev} of −69 and −63 mV, respectively), they were easily distinguished from glutamate receptor-mediated excitatory postsynaptic currents on the basis of their slower time course and their complete inhibition by 20 μM bicuculline (Ascent Scientific-Abcam). The currents recorded in the presence of bicuculline were subtracted to all records to obtain the evoked IPSCs (displayed in the figures after blanking 1–3 ms around each stimulus artefact for clarity). After IPSC stabilization (typically 3 minutes after break-in), 5–10 sweeps were averaged to obtain the IPSC amplitude. A liquid junction potential (LJP) of −8 mV should be added to all voltages to obtain the correct membrane potentials (Neher, 1992). Patch-clamp pipettes had resistances of 1.8–2.5 MΩ.

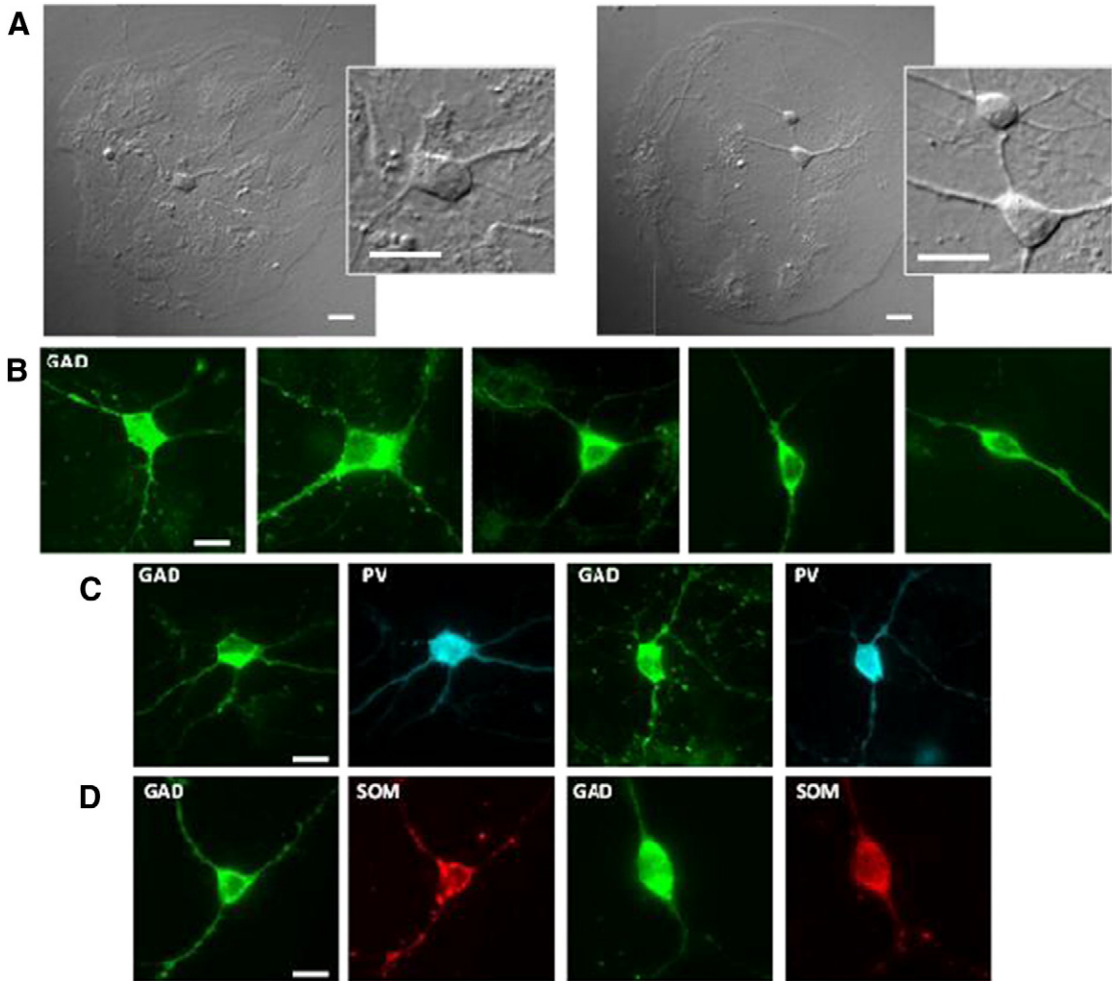

Fig. 1. Single cortical multipolar interneurons grown on glial microislands were selected for investigation of inhibitory autaptic neurotransmission. A. Left panel: representative picture under Nomarski optics of a microisland containing several glial cells and a single multipolar neuron with irregular soma morphology and multiple asymmetrical processes emanating from it (which is magnified in the inset), similar to those selected for recordings. Scale bar: 20 μm. Right panel: microisland containing several glial cells and two neurons, one representative of the neurons with ovoid soma morphology and symmetrical processes that were not considered for recordings and one representative of the multipolar neurons (that were used for recordings when they were the only neuron in the microisland). B. Representative pictures of different types of interneurons in microculture immunostained for GAD67: the three panels on the left show different multipolar interneurons representing the morphologies that were selected for recordings; the two panels on the right show interneurons with fusiform, ovoid or spindle-shaped soma and symmetrical processes that were not considered for recording. Scale bar: 10 μm. C. Representative pictures of interneurons in microculture immunostained for both GAD67 and parvalbumin (PV) in dual labeling experiments. The PV + interneurons have multipolar morphologies similar to those selected for recordings. Scale bar: 10 μm. D. Representative pictures of interneurons in microculture immunostained for both GAD67 and somatostatin (SOM) in dual labeling experiments. Sixty-one percent of SOM + interneurons had fusiform, ovoid or spindle shaped soma (right panel); 39% of SOM + interneurons had multipolar morphology similar to that of some of the cells selected for recordings (left panel). In triple labeling experiments, none of the neurons were positive for both PV and SOM. Scale bar: 10 μm.

The relative number of neurons recorded from WT and KI mice at different DIVs was closely matched.

The firing properties of neurons in microculture were studied with current clamp recordings (sampling 50 KHz; filter 10 KHz), in which baseline current injection was usually applied to maintain the resting potential near −70 mV and either long (1 s) depolarizing current pulses of increasing amplitude or short (20 ms) depolarizing current pulses were applied to elicit multiple and single action potentials (APs), respectively.

Acute thalamocortical slices of the barrel cortex were prepared from P11-13 mice as described in Tottene et al. (2009), and the firing properties of layer 2/3 FS interneurons were measured by applying (1 s long) suprathreshold current injections of increasing amplitude as in Tottene et al. (2009).

Action potential half width (AP_{hw}) was measured as the width of the AP at half maximal height (defined as the amplitude from AP voltage threshold to AP peak), considering the first AP in the train at rheobase current injection. The after-hyperpolarization (AHP) amplitude was measured as the difference between AP voltage threshold and the depth of the AHP. The frequency of APs was measured from the average of the last three interspike intervals, and the accommodation ratio as the ratio of the first to the mean of the last three interspike intervals after 600 ms during current pulses at 2–3 times the rheobase.

Whole-cell voltage-clamp recordings of Ca currents were performed on single neurons in microculture (DIV 6-9) with the same morphology as those selected for recording of evoked IPSCs. The pipette solution contained (in mM): 100 $CsCH_3SO_3$, 5 $MgCl_2$, 30 HEPES, 10 EGTA, 4 ATP, 0.5 GTP, 1 cAMP, pH 7.4 with CsOH. The extracellular solution contained (in mM) 5 $BaCl_2$, 148 TEA-Cl, 10 HEPES, 0.1 mg/ml cytochrome C, pH 7.4 with TEA-OH. LJP = −12 mV. Pharmacological dissection of the different Ca current components was performed using nimodipine (from Tocris) and the peptide toxins: ω-AgaIVA (from Peptide Institute Inc.), ω-CgTxGVIA, ω-CTxMVIIC (both from Bachem).

Data are given as mean ± SEM; stars indicate a statistically significant difference from control assessed by the unpaired or paired Student's *t* test, unless otherwise specified (*, $p < 0.05$; **, $p < 0.01$; ***, $p < 0.001$).

Results

Single cortical neurons grown on glial microislands form synaptic connections onto themselves (autapses) with properties very similar

to those of synapses between neurons (Bekkers and Stevens, 1991). We investigated inhibitory autaptic neurotransmission in microcultures of cortical neurons from neonatal wild-type (WT) and R192Q knockin (KI) mice. Given the well known large diversity of cortical interneurons (Petilla Interneuron Nomenclature Group, 2008; Rudy et al., 2011), to limit the heterogeneity, the recordings were performed only on cells characterized by irregular soma morphology with multiple asymmetrical processes emanating from it (multipolar interneurons) (cf Methods and Fig. 1). The recorded cells were enriched in fast-spiking (FS) interneurons relative to other types of interneurons because current clamp recordings revealed the high-frequency non-accommodating firing typical of FS interneurons in 62% (24 out of 39) of the cells (Fig. 2A). These interneurons had a mean firing frequency of 53 ± 3 Hz (with current injections 2 to 3 times the rheobase) and an accommodation ratio of 1.01 ± 0.06 ($n = 22$). Typically FS interneurons display brief action potentials (APs) with large amplitude fast afterhyperpolarization (AHP); the AP half width (AP_{hw}) is age- and temperature-dependent decreasing with both age and temperature (Ali et al., 2007; Goldberg et al., 2011). The FS interneurons in our DIV 10-13 microcultures had on average an AP_{hw} of 1.03 ± 0.04 ms and an AHP of 25 ± 1 mV ($n = 24$) at room temperature (Fig. 2A), which are consistent with the AP properties of FS interneurons in acute cortical slices from juvenile mice. In fact, we obtained similar values of AP duration and AHP from room temperature current clamp recordings of FS interneurons in acute thalamocortical slices of P11-13 WT ($AP_{hw} = 0.87 \pm 0.07$ ms; AHP = 21 ± 1 mV; $n = 11$) and R192Q KI mice ($AP_{hw} = 1.00 \pm 0.06$ ms; AHP = 22 ± 1 mV; $n = 11$).

Possibly, the fraction of FS interneurons derived from current clamp recordings is an underestimation because three interneurons classified as non-FS showed a single (or maximum two) AP of short duration (0.83 ± 0.16 ms) with a very deep AHP (35 ± 2 mV) at all current injections. To our knowledge similar firing properties have not been reported for interneurons in cortical slices and might be a consequence of the autaptic connections in microculture; if these cells are considered as modified FS interneurons, then the fraction of FS interneurons in the recorded cells increases to 69%.

Large inhibitory postsynaptic currents (IPSCs) were evoked in single cortical multipolar interneurons by brief depolarizing voltage steps eliciting an AP in the unclamped axonal processes (Fig. 2B). As previously shown for inhibitory synaptic transmission between layer 2/3 FS interneurons and pyramidal cells in cortical slices (Tottene et al., 2009), autaptic inhibitory neurotransmission in multipolar interneurons in microculture was unaltered in FHM1 KI mice. The average amplitude of the IPSC evoked in WT and KI interneurons was similar (Fig. 2B: 1.2 ± 0.1 nA, $n = 63$, in WT versus 1.1 ± 0.1 nA, $n = 53$, in KI; $p = 0.64$), despite the fact that P/Q-type Ca channels strongly contribute to control GABA release at the inhibitory autapses, as shown by the large fraction of the IPSC inhibited by the specific blocker ω-AgaIVA (200 nM) in most cells (Fig. 2C). Consistent with and further supporting the lack of effect of the FHM1 mutation on inhibitory autaptic transmission, ω-AgaIVA inhibited a similar fraction of the IPSC at WT and KI autapses (62 ± 6%, $n = 17$, in WT; 69 ± 8%, $n = 12$, in KI; $p = 0.319$, Wilcoxon test). As a likely reflection of the heterogeneity of the recorded multipolar interneurons and/or the heterogeneity of the Ca_V channels controlling release at FS interneuron synapses in different cortical areas (Ali and Nelson, 2006; Zaitsev et al., 2007; Kruglikov and Rudy, 2008; Tottene et al., 2009), the fractional inhibitions by ω-AgaIVA in one KI and one WT interneuron (< 20%) were outside the normal

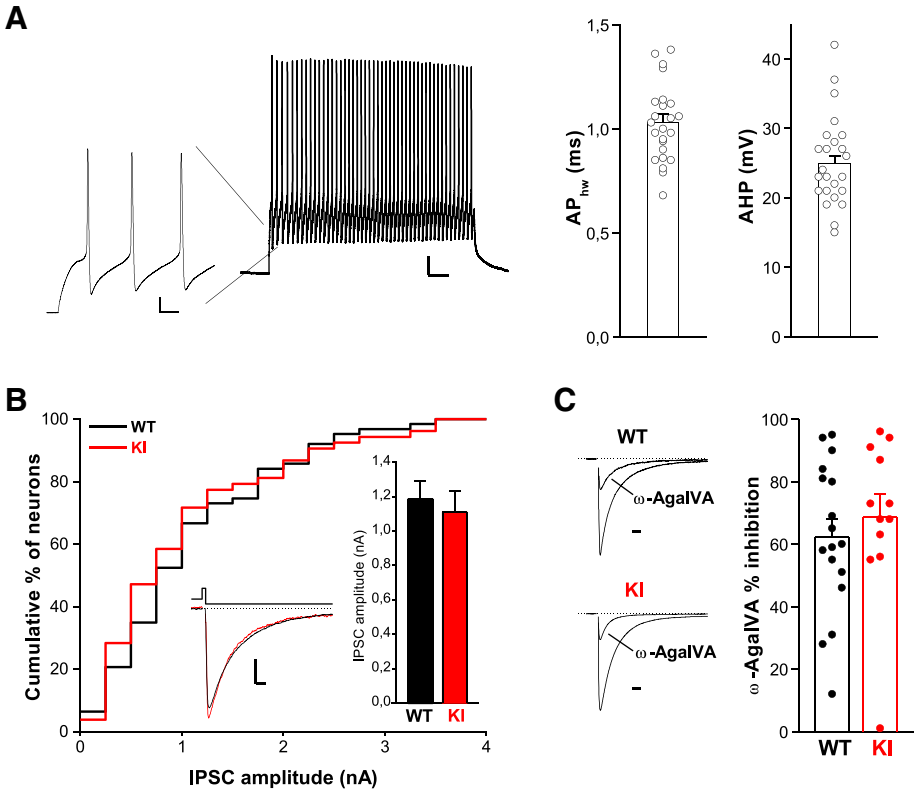

Fig. 2. Unaltered evoked IPSC amplitude and unaltered contribution of P/Q-type Ca channels to inhibitory neurotransmission at cortical multipolar (mainly FS) interneuron autapses of FHM1 KI mice. A. Left panel: representative current clamp trace showing the typical fast-spiking firing recorded in 24 out of 39 multipolar interneurons in microculture (DIV 10-13); scale bars: 100 ms (10 ms inset), 10 mV. The AP half width (AP_{hw}) and the AHP measured at rheobase current injection in these neurons are shown on the right. B. Cumulative distribution and average value (right inset) of IPSC amplitudes evoked in single WT ($n = 63$) and R192Q KI ($n = 53$) cortical multipolar interneurons in microculture (DIV 10-14). Left inset: representative IPSC traces from a WT (black) and KI (red) neuron; scale bars: 10 ms, 250 pA. C. Contribution of P/Q-type Ca channels to inhibitory autaptic neurotransmission evaluated from the fraction of the evoked IPSC inhibited by ω-AgaIVa (200 nM, a saturating concentration since the IPSC was not further inhibited by 400 nM ω-AgaIVA, $n = 4$ not shown) in WT ($n = 17$) and KI ($n = 12$) cortical multipolar interneurons in microculture; representative IPSC traces before and after ω-AgaIVa (normalized to the control value) are shown on the left (scale bar: 10 ms).

distribution; if one excludes these values, the average inhibition by ω-AgaIVA of autaptic inhibitory transmission increases, remaining similar in WT and KI mice (65 ± 5%, $n = 16$, in WT; 75 ± 5%, $n = 11$, in KI; $p = 0.204$).

Thus, the conclusion that the FHM1 mutation does not affect inhibitory neurotransmission at the synapses between layer 2/3 FS interneurons and pyramidal cells can be extended to the inhibitory autapses of cortical FS interneurons and, likely, to inhibitory autapses of other types of multipolar interneurons.

Given the low coefficient of variation of the unitary IPSPs and the close to zero percentage of failures at the connection between layer 2/3 FS interneurons and pyramidal cells, which is consistent with a high probability of AP-evoked GABA release at the active zones, Tottene et al. (2009) suggested saturation of the presynaptic Ca sensor as a possible explanation for the unaltered inhibitory neurotransmission in FHM1 KI mice despite the dominant role of P/Q-type Ca channels at these FS interneuron synapses. To investigate whether saturation of the presynaptic Ca sensor underlies the unaltered neurotransmission at the inhibitory autapses of cortical multipolar (mostly FS) interneurons, we measured the dependence of the evoked IPSC on the concentration of extracellular Ca ions ($[Ca^{2+}]_{out}$) in WT and FHM1 KI inhibitory autapses.

In comparison with the $[Ca^{2+}]_{out}$-dependence of the evoked EPSC at the excitatory autapses of WT cortical pyramidal cells (Tottene et al., 2009), the $[Ca^{2+}]_{out}$-dependence of the evoked IPSC at the inhibitory autapses of WT multipolar interneurons was shifted to lower $[Ca^{2+}]_{out}$ (EC_{50}: 1.00 ± 0.09 mM, $n = 9$, for inhibitory autapses versus 1.65 ± 0.1 mM, $n = 7$, for excitatory autapses; $p = 0.0003$) (Fig. 3A). As a consequence of the increased AP-evoked Ca influx through presynaptic P/Q-type Ca channels, the evoked EPSC at cortical pyramidal cell autapses of R192Q KI mice (at 2 mM Ca) was 1.7 times larger than that at WT autapses (Tottene et al, 2009), which corresponds to the maximal increment predicted by the Ca-dose response curve (in which the maximal EPSC is 1.7 times larger than the EPSC at 2 mM $[Ca^{2+}]_{out}$) (Fig. 3A). In contrast, at the inhibitory autapses the maximal value of the evoked IPSC is only 1.19 times larger than the IPSC at 2 mM $[Ca^{2+}]_{out}$, which is consistent with near saturation of the Ca^{2+} sensor at the $[Ca^{2+}]_{out}$ used in our experiments (Fig. 3A). This is confirmed by the ratio between the IPSCs evoked at 4 and 2 mM $[Ca^{2+}]_{out}$ in 23 multipolar interneurons, Ca4/Ca2 = 1.12 ± 0.03, which is similar to the value of

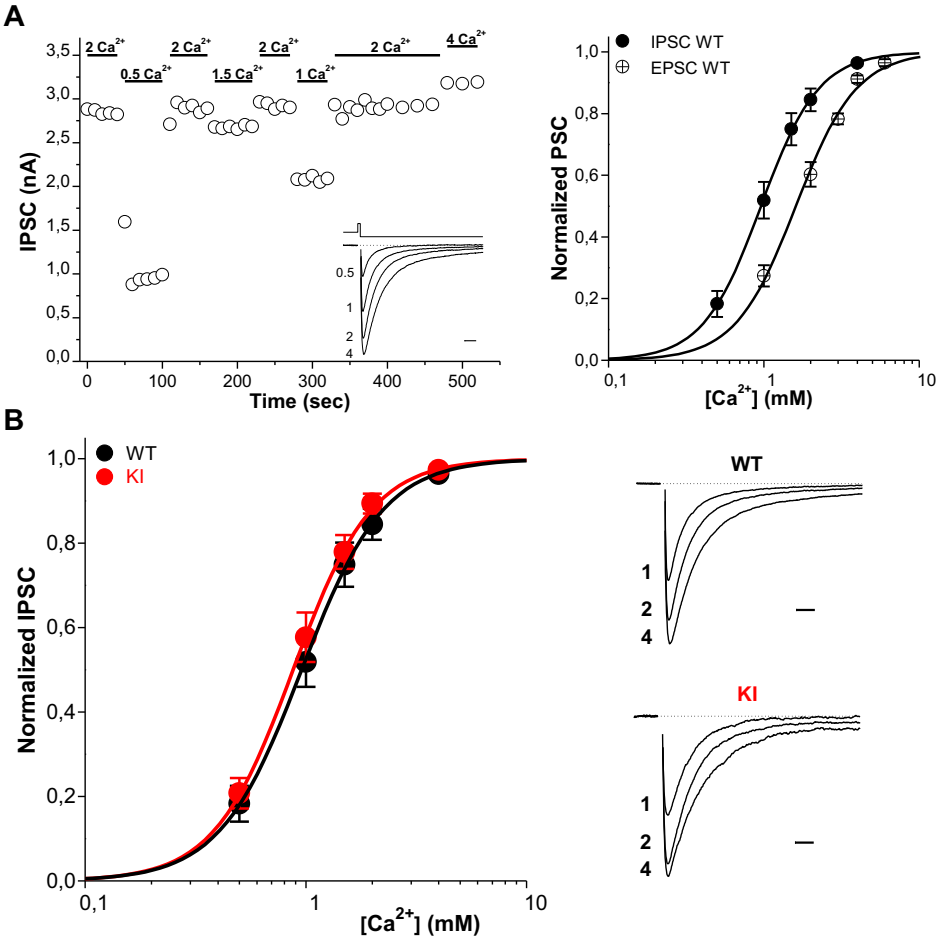

Fig. 3. Unaltered dependence of evoked IPSC on extracellular $[Ca^{2+}]$ at cortical multipolar interneuron autapses of FHM1 KI mice. A. Left panel: IPSC peak amplitudes against time during application of extracellular solutions with different Ca^{2+} concentrations, as indicated by the horizontal bars, in a representative experiment. Inset: IPSC traces recorded at the indicated $[Ca^{2+}]_{out}$ (in mM) and normalized to the value at 4 mM $[Ca^{2+}]_{out}$; scale bar 10 ms. Right panel: normalized amplitudes of IPSCs evoked in WT cortical multipolar interneurons (●) and of EPSCs evoked in WT cortical pyramidal cells in microculture (○) as a function of extracellular $[Ca^{2+}]$. The EPSC data points (shown for comparison) are taken from Tottene et al. (2009). In each cell, the PSC data points were fitted according to the Hill equation: $PSC = PSC_{max}([Ca^{2+}]^n/\{(EC_{50})^n + [Ca^{2+}]^n\})$ and the PSC amplitudes were then normalized to the PSC_{max} obtained from the fit. The average normalized PSC data points across cells ($n = 9$ for IPSC, $n = 7$ for EPSC) shown in the right panel were fitted with $EC_{50} = 0.96 \pm 0.01$ mM, $n = 2.21 \pm 0.04$ for IPSCs and $EC_{50} = 1.61 \pm 0.05$ mM, $n = 2.31 \pm 0.14$ for EPSCs. B. Left panel: normalized IPSC amplitudes as a function of extracellular $[Ca^{2+}]$ evoked in multipolar interneurons in microculture from WT ($n = 9$) and R192Q KI mice ($n = 8$). Average IPSC amplitudes at 2 mM $[Ca^{2+}]_{out}$: 1.1 ± 0.3 nA (WT, $n = 9$) and 1.0 ± 0.3 nA (KI, $n = 8$). The data points are fitted according to the equation $IPSC = [Ca^{2+}]^n/\{(EC_{50})^n + [Ca^{2+}]^n\}$ with $EC_{50} = 0.96 \pm 0.01$ mM, $n = 2.34 \pm 0.04$ for WT and $EC_{50} = 0.88 \pm 0.01$ mM, $n = 2.43 \pm 0.05$ for KI. Right panel: normalized IPSC traces recorded at the indicated $[Ca^{2+}]_{out}$ (in mM) from a WT and KI neuron; scale bar 10 ms.

1.14 ± 0.04 from the 9 cells in which we obtained the complete Ca-dose response curve. Assuming that the FHM1 mutation does increase AP-evoked Ca influx through P/Q-type Ca channels at the inhibitory autapses, one expects, at most, a 19% increase of the evoked IPSC in R192Q KI mice. Such a small increase might have escaped detection due to experimental variability. However, if indeed near saturation of the Ca sensor underlies the similar evoked IPSCs at WT and mutant autapses, one expects to reveal gain-of-function of inhibitory autaptic transmission by lowering $[Ca^{2+}]_{out}$, and one predicts that the Ca^{2+} dependence of the IPSC should be shifted to lower $[Ca^{2+}]_{out}$ in R192Q KI compared to WT mice [as found at excitatory pyramidal cell autapses by Tottene et al. (2009)].

In contrast with this prediction, the evoked IPSC at WT and mutant autapses showed a similar dependence on $[Ca^{2+}]_{out}$ (EC_{50}: 0.91 ± 0.08 mM, $n = 8$, for KI autapses versus 1.0 ± 0.09 mM, $n = 9$, for WT multipolar interneuron autapses, $p = 0.44$) and similar amplitudes at each $[Ca^{2+}]_{out}$ (Fig. 3B), implying similar AP-evoked Ca influx at the active zones of the inhibitory autapses of WT and R192Q KI mice. We therefore conclude that the unaltered inhibitory autaptic transmission in the FHM1 mouse model is due to unaltered AP-evoked Ca influx through presynaptic P/Q-type Ca channels at multipolar (mostly FS) interneuron autapses rather than to near saturation of the presynaptic Ca sensor.

Unaltered AP-evoked Ca current at calyx of Held synaptic terminals of R192Q KI mice, despite a shifted activation to lower voltages of mutant calyx presynaptic $Ca_V2.1$ channels similar to that of mutant channels in cortical pyramidal cells, has been recently reported (Inchauspe et al., 2010). It has been shown that the (about four times) shorter duration of the AP in Calyx terminals than in pyramidal cells could largely explain the differential effect of the FHM1 mutation on AP-evoked Ca current at cortical pyramidal cell and Calyx synapses (Inchauspe et al., 2010), leading to the suggestion that the short duration of the AP in FS interneurons could similarly result in unaltered AP-evoked Ca current at FS interneuron synapses and thus explain the unaltered synaptic transmission at FS interneuron-pyramidal cell synapses reported by Tottene et al. (2009).

To investigate whether the relatively short duration of the AP explains the lack of effect of the FHM1 mutation on AP-evoked Ca influx at the multipolar (mainly FS) interneuron inhibitory autapses, we prolonged the duration of the AP using tetraethylammonium (TEA, 10 mM) and measured evoked IPSCs at 1, 2 and 4 mM $[Ca^{2+}]_{out}$ in the presence of TEA in WT and R192Q KI multipolar interneurons. If a gain-of-function of AP-evoked Ca influx due to activation of mutant presynaptic $Ca_V2.1$ channels at lower voltages than WT channels is prevented by the relatively short AP duration, one expects that prolongation of the AP should uncover the gain-of-function, resulting in a shift to lower voltages of the $[Ca^{2+}]_{out}$-dependence of the IPSC and a corresponding increase of the IPSC at 1 mM $[Ca^{2+}]_{out}$ (far from saturation) in KI compared to WT inhibitory autapses.

The average increase in AP duration, AP_{hw}, produced by TEA in individual multipolar interneurons was 35 ± 7% ($n = 10$; from 0.87 ± 0.08 ms to 1.21 ± 0.18 ms, $p = 0.007$), accompanied by a decrease in the AHP amplitude of 57 ± 8% ($n = 9$; from 26 ± 2 to 12 ± 3 mV, $p = 0.0001$). The prolongation of the AP resulted in a 44 ± 5% average increase of the evoked IPSC at 1 mM $[Ca^{2+}]_{out}$ ($n = 16$) (Fig. 4).

Evoked IPSCs in the presence of TEA at 1, 2 and 4 mM $[Ca^{2+}]_{out}$ were measured in WT and R192Q KI multipolar interneurons using the protocol shown in Fig. 5A. The similar values of the average WT and KI IPSCs (normalized to the value at 4 mM $[Ca^{2+}]_{out}$ in each cell: 0.72 ± 0.04, $n = 14$, in WT; 0.77 ± 0.04, $n = 11$, in KI at 1 mM $[Ca^{2+}]_{out}$, $p = 0.34$) (Fig. 5B) show that prolongation of the AP does not uncover gain-of-function of inhibitory neurotransmission at multipolar interneuron autapses. We therefore conclude that the unaltered AP-evoked Ca influx through presynaptic P/Q-type Ca channels at multipolar (mostly FS) interneuron autapses and the unaltered inhibitory autaptic transmission in the FHM1 mouse model is not due to the relatively short AP duration in the interneurons.

Fioretti et al. (2011) have shown that the gating properties of the specific $Ca_V2.1$ channels expressed in capsaicin-sensitive trigeminal ganglion neurons of R192Q KI mice are not affected by the FHM1 mutation. Accordingly, CGRP release from the peripheral terminals of trigeminal dural afferents was unaltered in the FHM1 KI mice. It seems then possible that the expression in cortical multipolar interneurons of specific $Ca_V2.1$ channels whose gating properties are not affected by the FHM1 mutation may similarly underlie the unaltered inhibitory transmission at the interneuron autapses of R192Q KI mice. To investigate this possibility, we measured the whole-cell P/Q-type Ca current density as a function of voltage in single cortical multipolar interneurons grown on glial microislands. The P/Q-type Ca^{2+} current component was obtained as the amount of current inhibited by either ω-conotoxin MVIIC (MVIIC, 3 μM) or ω-AgaIVA (200 nM), applied after sequential additions of nimodipine (5 μM) and ω-conotoxin GVIA (GVIA, 1 μM) to inhibit L-

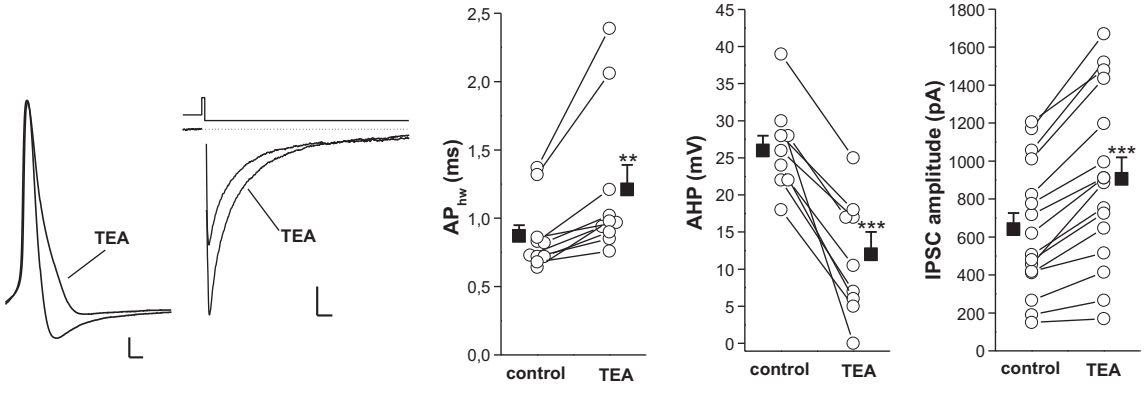

Fig. 4. TEA prolongs the duration of the action potential in cortical multipolar (mainly FS) interneurons in microculture and increases the evoked IPSC. The representative traces on the left show single APs induced by a 20-ms long near rheobase current injection and IPSCs evoked in a multipolar interneuron in control solution (with 1 mM $[Ca^{2+}]_{out}$) and in the presence of TEA (10 mM); scale bars: 1 ms, 10 mV and 10 ms, 100 pA. TEA prolongs the AP and decreases the AHP amplitude as quantified in the right panels showing the values of AP_{hw} and AHP in 10 individual multipolar interneurons (DIV 10-13) together with the corresponding average values in control and in the presence of TEA. Seven of these multipolar interneurons were FS or "modified FS" (showing only one or two brief APs) neurons and showed a larger prolongation of the AP by TEA (44 ± 7%, $n = 7$) compared to non-FS interneurons (14 ± 2%, $n = 3$).TEA increases the evoked IPSC amplitude as quantified in the third right panel showing the IPSC amplitudes in 16 individual multipolar interneurons (DIV 10-13) together with the corresponding average values in control and in the presence of TEA ($p = 0.000002$). In five of these interneurons current- and voltage-clamp experiments were performed on the same cell, thus allowing correlations between firing properties, increase in AP duration by TEA and increase in IPSC consequent to the AP prolongation. Four of these multipolar interneurons were FS or "modified FS" interneurons and showed a larger increase of IPSC by TEA (65 ± 13%, in correlation with an average prolongation of the AP by 45 ± 7%; $n = 4$) compared to the non-FS multipolar interneuron (23%, in correlation with a smaller prolongation of the AP of 18%).

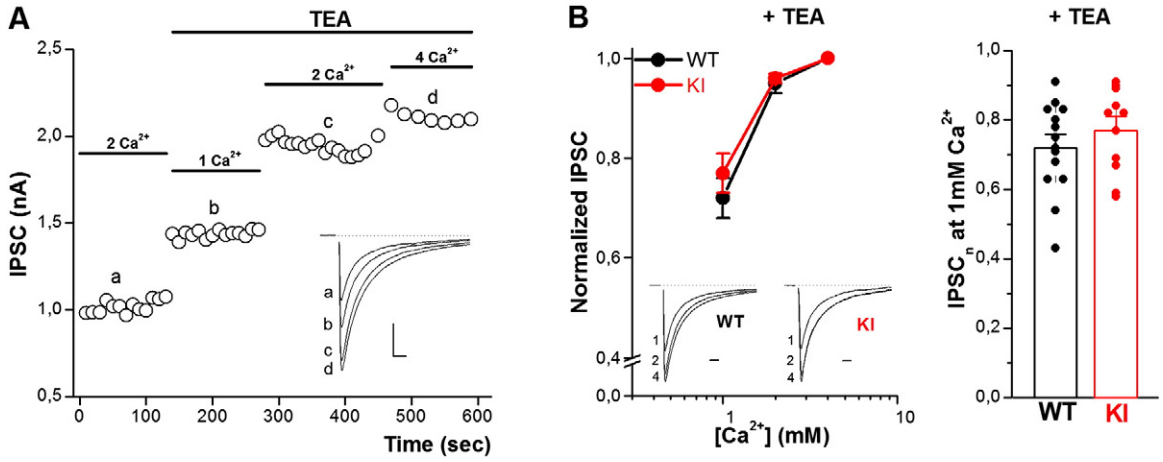

Fig. 5. Prolongation of the AP with TEA does not uncover gain-of-function of inhibitory neurotransmission at multipolar interneuron autapses. A. IPSC peak amplitudes against time during application of extracellular solutions with 1, 2, 4 mM $[Ca^{2+}]$ and TEA (10 mM), as indicated by the horizontal bars, in a representative experiment. Inset: IPSC traces recorded at times a, b, c, d; scale bar 10 ms, 500 pA. B. Left panel: normalized amplitudes of IPSCs evoked in WT ($n = 14$) and R192Q KI ($n = 11$) cortical multipolar interneurons as a function of extracellular $[Ca^{2+}]$ in the presence of TEA; the IPSC amplitudes were normalized to the value at 4 mM $[Ca^{2+}]_{out}$ in each cell and then averaged. Inset: normalized IPSC traces recorded in a WT and a KI multipolar interneuron in the presence of TEA at the indicated $[Ca^{2+}]_{out}$ (in mM); scale bar 10 ms. Right panel: normalized IPSC amplitudes in WT ($n = 14$) and R192Q KI ($n = 11$) multipolar interneurons in the presence of TEA with 1 mM $[Ca^{2+}]_{out}$ ($p = 0.34$).

and N-type Ca channels, respectively (Fig. 6A). In the large majority of WT multipolar interneurons (29 out of 33: 88%) the P/Q-type Ca current was the largest pharmacological component amounting to 36 ± 2% of the total Ca current (53 ± 2% of the non L-type Ca current) (Fig. 6B). Twelve percent of multipolar interneurons did not have a measurable P/Q-type Ca current, a fraction comparable to that of the interneurons showing a small (< 20%) contribution of P/Q-type Ca channels to inhibitory autaptic neurotransmission.

Fitting of the current–voltage (*I-V*) relationships of the P/Q-type Ca current in individual WT and KI multipolar interneurons gave mean half activation voltages of −9.8 ± 1.1 mV ($n = 12$) and −13.1 ± 0.8 mV (n = 14), respectively ($p = 0.02$) (Fig. 6C). The small shift to more negative voltages of the P/Q-type Ca current activation in KI compared to WT interneurons (much smaller than that measured in cortical pyramidal cells, shown for comparison in Fig. 6D) did not result in significantly larger P/Q-type Ca current densities in KI interneurons ($p = 0.532$, one-way ANOVA for repeated measures test; Fig. 6C), in contrast with the significantly larger P/Q-type Ca current densities in KI compared to WT pyramidal cells (Tottene et al, 2009). The L-, N- and R-type Ca current densities were also similar in WT and KI multipolar interneurons (at 0 mV, L-type: 11 ± 1 pA/pF versus 11.4 ± 0.9 pA/pF; N-type: 4.3 ± 0.7 pA/pF versus 6.3 ± 0.8 pA/pF; R-type: 6.1 ± 0.5 pA/pF versus 7 ± 2 pA/pF; P/Q- type: 11.7 ± 0.8 pA/pF versus 12.5 ± 1.2 pA/pF; $n = 17$ for WT and $n = 18$ for KI; $p = 0.92$, 0.07, 0.55 and 0.6, respectively), thus confirming the absence of compensatory changes found in other types of neurons (Fioretti et al., 2011; Tottene et al., 2009; van den Maagdenberg et al., 2004).

We conclude that the current density and the gating properties of the $Ca_V2.1$ channels expressed by multipolar interneurons are barely affected by the FHM1 mutation, thus providing an explanation for the unaltered AP-evoked Ca influx through P/Q-type Ca channels at the multipolar interneuron autapses and the unaltered autaptic inhibitory neurotransmission in FHM1 KI mice.

Discussion

Our analysis of inhibitory neurotransmission in microcultures of cortical neurons from WT and FHM1 R192Q KI mice has shown that the FHM1 mutation does not affect inhibitory transmission at autapses of cortical FS (and other types of multipolar) interneurons, despite a dominant role of P/Q-type Ca channels in controlling GABA release. This confirms and extends our previous finding of unaltered inhibitory synaptic transmission between layer 2/3 FS interneurons and pyramidal cells in acute slices of R192Q KI mice (Tottene et al., 2009).

We have investigated several mechanisms that were suggested as possible explanations for the unaltered inhibitory transmission at FS interneuron synapses despite a dominant role of P/Q-type channels in controlling GABA release, namely: (i) saturation of the presynaptic Ca sensor (Tottene et al., 2009); (ii) short duration of the AP in FS interneurons leading to unaltered AP-evoked presynaptic Ca influx despite shifted activation of mutant $Ca_V2.1$ channels to lower voltages (Inchauspe et al., 2010; Inchauspe et al., 2012; Tottene et al., 2009); and (iii) interneuron-specific $Ca_V2.1$ channels whose gating properties are not (or barely) affected by the FHM1 mutation (Fioretti et al., 2011; Tottene et al., 2009; Xue and Rosenmund, 2009).

We have shown that the unaltered inhibitory transmission at multipolar interneuron autapses in the FHM1 mouse model is due to unaltered AP-evoked Ca influx through presynaptic $Ca_V2.1$ channels and not to near saturation of the presynaptic Ca sensor, since lowering $[Ca]_{out}$ did not reveal a gain-of-function of evoked transmission (Fig. 3). Gain-of-function of inhibitory transmission at low $[Ca]_{out}$ was not uncovered even after prolongation of the AP with TEA (Fig. 5), indicating that the unaltered AP-evoked Ca influx through presynaptic $Ca_V2.1$ channels is not due to the relatively short duration of the AP in multipolar (mostly FS) interneurons. In contrast with the shifted activation to lower voltages of mutant P/Q-type Ca channels in pyramidal cells and other CNS excitatory neurons (Inchauspe et al., 2010; Tottene et al., 2009; van den Maagdenberg et al., 2004), the gating properties of the P/Q-type Ca channels expressed in cortical multipolar interneurons in microculture were barely affected by the FHM1 mutation. These findings support the conclusion that the lack of effect of the FHM1 mutation on inhibitory neurotransmission at multipolar (mainly FS) interneuron autapses may be explained by the expression in these interneurons of specific $Ca_V2.1$ channels whose gating is barely affected by the FHM1 mutation.

Most likely, this explains also the lack of effect of the FHM1 mutation on inhibitory synaptic transmission at FS interneuron synapses in cortical slices. In fact, given the age dependence of AP duration in FS interneurons (Goldberg et al., 2011), at the age (P11-13) when unaltered inhibitory transmission at unitary layer 2/3 FS interneuron-pyramidal cell synapses was described (Tottene et al., 2009), the AP duration measured in layer 2/3 FS interneurons in cortical slices (AP_{hw}: 0.94 ± 0.05 ms, $n = 22$, at room temperature) is similar to that measured in multipolar interneurons in microculture (AP_{hw}: 1.03 ± 0.04 ms; p =

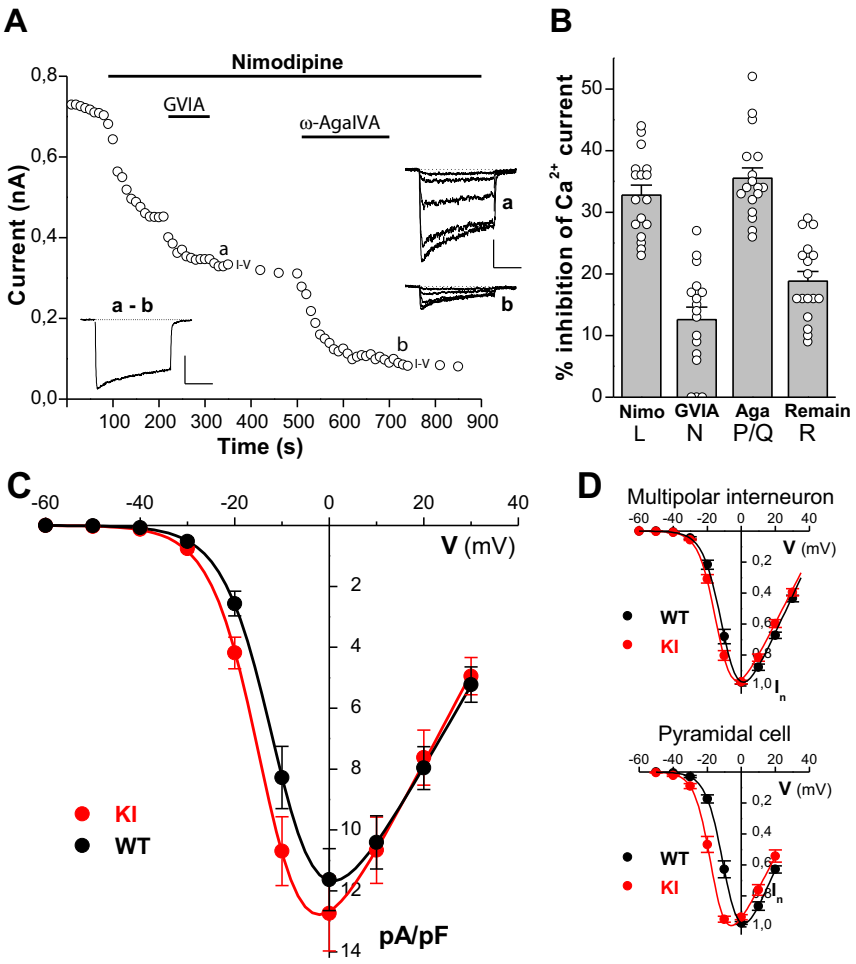

Fig. 6. The gating properties of the $Ca_V2.1$ channels expressed in multipolar interneurons are barely affected by the FHM1 mutation. A. Peak whole-cell Ba^{2+} current versus time recorded from a DIV 9 multipolar interneuron in microculture during depolarizations at 0 mV every 10 s from holding potential of −70 mV before and after sequential application of the indicated drugs (applied for the time indicated by the horizontal bars). Insets: on the left, representative P/Q-type current trace obtained as the difference between traces at times a and b; on the right, representative traces at increasing voltage from −40 to 0 mV, taken during current–voltage (*I-V*) measurements at times a and b. Scale bars: 50 ms, 100 pA. B. Contribution of the L-, N-, P/Q-, and R-type Ca current components in DIV 6-9 WT multipolar interneurons ($n = 17$), as obtained from the percentage of whole-cell Ba^{2+} current (at 0 mV) inhibited by nimodipine, GVIA, MVIIC or ω-AgaIVA (Aga) and remaining (in the presence of nimodipine after subsequent applications of GVIA and Aga), respectively. Only interneurons with P/Q-type Ca current for which all four pharmacological components could be measured were included ($n = 17$). Out of a total of 33 recorded multipolar interneurons, four (12%) did not show any P/Q-type Ca current; in these interneurons an increased fractional contribution of N-type Ca current (42 ± 4%) compensated for the lack of P/Q-type current; the fractional contribution of the L- and R-type components were 38 ± 4% and 20 ± 3%, respectively, similar to those in P/Q-expressing interneurons. C. P/Q-type current density as a function of voltage in WT ($n = 12$) and KI ($n = 14$) multipolar interneurons in microculture. Lines are fits of the equation $I = G(V - E_{rev})(1 + \exp[(V_{1/2} - V)/k])^{-1}$ with $V_{1/2} = -10.3 \pm 0.1$ mV ($k = 5.3 \pm 0.04$ mV) and $V_{1/2} = -13.1 \pm 0.2$ mV ($k = 5.2 \pm 0.1$ mV) for WT and KI, respectively. D. Normalized P/Q-type current densities as a function of voltage in WT ($n = 12$) and KI ($n = 14$) multipolar interneurons in microculture and in WT ($n = 10$) and KI ($n = 9$) dissociated cortical pyramidal cells (Tottene et al., 2009). Fitting the *I-V* curves for cortical pyramidal cells gave $V_{1/2} = -8.0 \pm 1$ mV and $V_{1/2} = -16 \pm 1$ mV for WT and KI, respectively (Tottene et al., 2009).

0.140). At Calyx of Held synapses, APs of similar duration (about 1 ms half duration, in the presence of TEA) did reveal gain-of-function of AP-evoked Ca current and excitatory transmission due to the shifted activation gating of presynaptic $Ca_V2.1$ channels (in contrast with the lack of gain-of-function with the much shorter control APs of 0.44 ms half duration) (Inchauspe et al., 2010; Inchauspe et al., 2012). Similarly, in cortical pyramidal cells, gain-of-function of the AP-evoked Ca current was observed using as voltage stimulus APs of 0.93 ms half duration that were recorded at physiological temperature (Inchauspe et al., 2010).

Inhibition in the cortex is generated by a variety of different types of GABAergic interneurons, that can be subdivided in three non overlapping populations on the basis of the expression of PV, SOM and 5HT3a receptors (5HT3aR); each population is heterogeneous in terms of morphology and firing properties of the interneurons composing it, although to a different degree (Rudy et al., 2011). The large majority of PV + interneurons (the largest population of interneurons in the neocortex) shows FS non-adapting firing and irregular soma with multipolar dendritic morphology. In contrast, a large fraction of Martinotti cells, the SOM + interneurons that target the apical dendrites of pyramidal cells, and a fraction of 5HT3aR + interneurons show ovoid, fusiform or spindle-shaped soma with bitufted or bipolar dendritic morphology and various types of (regular or irregular) adapting firing (Rudy et al., 2011). To limit the heterogeneity, we measured autaptic neurotransmission and Ca currents only in interneurons with irregular soma and multiple asymmetrical processes emanating from it (multipolar interneurons) and not in interneurons with ovoid, fusiform or spindle-shaped soma and symmetrical processes. As expected, most (62–70%) multipolar interneurons were FS interneurons, but not all. The nature of the non-FS multipolar interneurons we recorded from remains unclear since both SOM + and 5HT3aR + interneurons comprise multipolar interneurons with regular adapting or irregular firing similar to that shown by non-FS interneurons in microculture. However, in three DIV 12 microcultures, only 33 out of a total of 483 GAD-positive neurons were SOM + (6.8%) and 13 of these SOM + interneurons were multipolar (data not shown); the small fraction of SOM

+ interneurons suggests that 5HT3aR + interneurons might represent the majority of the recorded non-FS multipolar interneurons.

In any case, the lack of effect of the FHM1 mutation on autaptic neurotransmission and Ca current in the heterogeneous population of multipolar interneurons in microculture point to the possibility that unaltered inhibitory synaptic transmission in FHM1 is a general property not limited to FS interneuron synapses. Indeed, we have preliminary evidence that the R192Q mutation does not affect synaptic transmission at unitary inhibitory connections between layer 2/3 SOM + interneurons and pyramidal cells (N. Pilati, M. Sessolo and D. Pietrobon, unpublished findings).

Overall, our findings suggest that expression of different $Ca_V2.1$ channels in inhibitory and excitatory cortical neurons may underlie the differential effect of the FHM1 mutation on inhibitory and excitatory synaptic transmission. While the molecular mechanisms underlying the differential modulation of the gating properties of the specific $Ca_V2.1$ channels expressed in excitatory and inhibitory cortical neurons remain unknown, possible mechanisms include the expression of different splicing variants of the α1 subunit (Adams et al., 2009) and/or the expression of different auxiliary subunits (Mullner et al., 2004) and/or other modulatory proteins (Catterall and Few, 2008). In this respect, it is interesting that inhibitory modulation by SNAP25 of the Ca current was observed in glutamatergic but not GABAergic hippocampal neurons in primary culture (Condliffe and Matteoli, 2011; Condliffe et al., 2010), and reduction of SNAP25 by siRNA knockdown or in $SNAP25^{-/+}$ mice resulted in reduced evoked inhibitory synaptic transmission [ascribed to the function of SNAP25 as component of the SNARE complex (Boyken et al., 2013; Tafoya et al., 2006)] but, in contrast, enhanced evoked excitatory synaptic transmission due to increased probability of glutamate release, which is consistent with reduced inhibition of presynaptic Ca channels by SNAP25 at excitatory synapses (Antonucci et al., 2013).

The evidence of cortical neuron subtype-specific alterations of $Ca_V2.1$ channels by FHM1 mutations presented here [and cf also the previous evidence of trigeminal ganglion neuron subtype-specific alterations in Fioretti et al. (2011)] has an important implication for familial migraine (and in general for channelopathies) mechanisms in that it may help to explain why a mutation in a Ca channel that is widely expressed in the nervous system (Westenbroek et al., 1995) produces the specific neuronal dysfunctions leading to migraine. It has been suggested that, as a consequence of the differential effect of the FHM1 mutations on synaptic transmission and short-term plasticity at different cortical synapses (noting the lack of effect at inhibitory synapses), the neuronal circuits that dynamically maintain a tight balance between excitation and inhibition during cortical activity are very likely altered in FHM1. Functional alterations in these circuits may underlie the abnormal processing of sensory information typical of migraineurs in the interictal period and, in certain conditions (e.g. in response to specific migraine triggers), lead to disruption of the excitatory/inhibitory balance and to neuronal hyperactivity, that may result in elevations of extracellular K^+ above the critical value for ignition of CSD (Pietrobon and Moskowitz, 2013; Tottene et al., 2009; Vecchia and Pietrobon, 2012).

Despite recent drug developments, there is a great need for more efficacious and specific prophylactic migraine medications. The finding of neuron subtype-specific alterations of $Ca_V2.1$ channel functioning by FHM1 mutations poses a challenge to future drug discovery aimed at counteracting excessive glutamatergic synaptic transmission in FHM and other migraine variants by targeting glutamatergic synapses without compromising inhibitory (and other normal) synapses (Vecchia and Pietrobon, 2012; Xue and Rosenmund, 2009).

Conclusions

In contrast with the increased current density and the left-shifted activation gating of the $Ca_V2.1$ channels in cortical pyramidal cells from R192Q FHM1 knockin mice, the current density and activation gating of the $Ca_V2.1$ channels expressed in cortical multipolar (mainly FS) interneurons in microculture are barely affected by the FHM1 mutation. This may explain the unaltered AP-evoked Ca influx and the consequent unaltered inhibitory neurotransmission at the autapses of these interneurons, that contrasts with the enhanced AP-evoked Ca influx and enhanced excitatory neurotransmission at cortical pyramidal cell synapses. Neither saturation of the presynaptic Ca sensor nor the relatively short duration of the interneuron AP can explain the unaltered AP-evoked Ca influx and the unaltered neurotransmission at the inhibitory autapses. Overall, our findings suggest that expression of different $Ca_V2.1$ channels in inhibitory and excitatory cortical neurons underlies the differential effect of FHM1 mutations on inhibitory and excitatory synaptic transmission and the likely consequent dysregulation of the cortical excitatory–inhibitory balance in FHM1.

Acknowledgments

This work was supported by Telethon Italy grant GGP06234 (to D.P.), the Italian Ministry of University and Research PRIN2007, 2010 (to D.P.), the University of Padova Strategic Project: Physiopathology of Signaling in Neuronal Tissue and Progetto Ateneo 2012 (to D.P.), the Centre for Medical Systems Biology (CMSB) in the framework of the Netherlands Genomics Initiative (NGI) (to A.M.J.M.v.d.M). Thanks to L. Broos for technical assistance.

References

Adams, P.J., Garcia, E., David, L.S., Mulatz, K.J., Spacey, S.D., Snutch, T.P., 2009. Ca(V)2.1 P/Q-type calcium channel alternative splicing affects the functional impact of familial hemiplegic migraine mutations: Implications for calcium channelopathies. Channels (Austin) 3, 110–121.

Ali, A.B., Nelson, C., 2006. Distinct Ca2 + channels mediate transmitter release at excitatory synapses displaying different dynamic properties in rat neocortex. Cereb. Cortex 16, 386–393.

Ali, A.B., Bannister, A.P., Thomson, A.M., 2007. Robust correlations between action potential duration and the properties of synaptic connections in layer 4 interneurones in neocortical slices from juvenile rats and adult rat and cat. J. Physiol. 580, 149–169.

Antonucci, F., Corradini, I., Morini, R., Fossati, G., Menna, E., Pozzi, D., Pacioni, S., Verderio, C., Bacci, A., Matteoli, M., 2013. Reduced SNAP-25 alters short-term plasticity at developing glutamatergic synapses. EMBO Rep. 14, 645–651.

Bekkers, J.M., Stevens, C.F., 1991. Excitatory and inhibitory autaptic currents in isolated hippocampal neurons maintained in cell culture. Proc. Natl. Acad. Sci. U. S. A. 88, 7834–7838.

Boyken, J., Gronborg, M., Riedel, D., Urlaub, H., Jahn, R., Chua, J.J., 2013. Molecular profiling of synaptic vesicle docking sites reveals novel proteins but few differences between glutamatergic and GABAergic synapses. Neuron 78, 285–297.

Brody, D.L., Yue, D.T., 2000. Release-independent short-term synaptic depression in cultured hippocampal neurons. J. Neurosci. 20, 2480–2494.

Catterall, W.A., Few, A.P., 2008. Calcium channel regulation and presynaptic plasticity. Neuron 59, 882–901.

Condliffe, S.B., Matteoli, M., 2011. Inactivation kinetics of voltage-gated calcium channels in glutamatergic neurons are influenced by SNAP-25. Channels (Austin) 5, 304–307.

Condliffe, S.B., Corradini, I., Pozzi, D., Verderio, C., Matteoli, M., 2010. Endogenous SNAP-25 regulates native voltage-gated calcium channels in glutamatergic neurons. J. Biol. Chem. 285, 24968–24976.

Fioretti, B., Catacuzzeno, L., Sforna, L., Gerke-Duncan, M.B., van den Maagdenberg, A.M., Franciolini, F., Connor, M., Pietrobon, D., 2011. Trigeminal ganglion neuron subtype-specific alterations of Ca(V)2.1 calcium current and excitability in a Cacna1a mouse model of migraine. J. Physiol. 589, 5879–5895.

Goldberg, E.M., Jeong, H.Y., Kruglikov, I., Tremblay, R., Lazarenko, R.M., Rudy, B., 2011. Rapid developmental maturation of neocortical FS cell intrinsic excitability. Cereb. Cortex 21, 666–682.

Inchauspe, C.G., Urbano, F.J., Di Guilmi, M.N., Forsythe, I.D., Ferrari, M.D., van den Maagdenberg, A.M., Uchitel, O.D., 2010. Gain of function in FHM-1 Ca(V)2.1 knock-in mice is related to the shape of the action potential. J. Neurophysiol. 104, 291–299.

Inchauspe, C.G., Urbano, F.J., Di Guilmi, M.N., Ferrari, M.D., van den Maagdenberg, A.M., Forsythe, I.D., Uchitel, O.D., 2012. Presynaptic CaV2.1 calcium channels carrying familial hemiplegic migraine mutation R192Q allow faster recovery from synaptic depression in mouse calyx of Held. J. Neurophysiol. 108, 2967–2976.

Kruglikov, I., Rudy, B., 2008. Perisomatic GABA release and thalamocortical integration onto neocortical excitatory cells are regulated by neuromodulators. Neuron 58, 911–924.

Levi, G., Aloisi, M., Ciotti, M., Gallo, V., 1984. Autoradiographic localization and depolarization-induced release of amino acids in differentiating granule cells cultures. Brain Res. 290, 77–86.

Mullner, C., Broos, L.A., van den Maagdenberg, A.M., Striessnig, J., 2004. Familial Hemiplegic Migraine Type 1 Mutations K1336E, W1684R, and V1696I Alter Cav2.1 Ca2 +

Channel Gating: Evidence for beta-subunit isoform-specific effects. J. Biol. Chem. 279, 51844–51850.
Neher, E., 1992. Correction for liquid junction potentials in patch clamp experiments. Methods Enzymol. 207, 123–131.
Ophoff, R.A., Terwindt, G.M., Vergouwe, M.N., van Eijk, R., Oefner, P.J., Hoffman, S.M.G., Lamerdin, J.E., Mohrenweiser, H.W., Bulman, D.E., Ferrari, M., Haan, J., Lindhout, D., van Hommen, G.-J.B., Hofker, M.H., Ferrari, M.D., Frants, R.R., 1996. Familial hemiplegic migraine and episodic ataxia type-2 are caused by mutations in the Ca^{2+} channel gene CACNL1A4. Cell 87, 543–552.
Petilla Interneuron Nomenclature Group, 2008. Petilla terminology: Nomenclature of features of GABAergic interneurons of the cerebral cortex. Nat. Rev. Neurosci. 9, 557–568.
Pietrobon, D., 2005. Function and dysfunction of synaptic calcium channels: Insights from mouse models. Curr. Opin. Neurobiol. 15, 257–265.
Pietrobon, D., 2010. CaV2.1 channelopathies. Pflugers Arch. 460, 375–393.
Pietrobon, D., Moskowitz, M.A., 2013. Pathophysiology of migraine. Annu. Rev. Physiol. 75, 365–391.
Rudy, B., Fishell, G., Lee, S., Hjerling-Leffler, J., 2011. Three groups of interneurons account for nearly 100% of neocortical GABAergic neurons. Dev. Neurobiol. 71, 45–61.
Tafoya, L.C., Mameli, M., Miyashita, T., Guzowski, J.F., Valenzuela, C.F., Wilson, M.C., 2006. Expression and function of SNAP-25 as a universal SNARE component in GABAergic neurons. J. Neurosci. 26, 7826–7838.
Tottene, A., Conti, R., Fabbro, A., Vecchia, D., Shapovalova, M., Santello, M., van den Maagdenberg, A.M.J.M., Ferrari, M.D., Pietrobon, D., 2009. Enhanced excitatory transmission at cortical synapses as the basis for facilitated spreading depression in Ca(v)2.1 knockin migraine mice. Neuron 61, 762–773.
van den Maagdenberg, A.M., Pietrobon, D., Pizzorusso, T., Kaja, S., Broos, L.A., Cesetti, T., van de Ven, R.C., Tottene, A., van der Kaa, J., Plomp, J.J., Frants, R.R., Ferrari, M.D., 2004. A Cacna1a knockin migraine mouse model with increased susceptibility to cortical spreading depression. Neuron 41, 701–710.
Vecchia, D., Pietrobon, D., 2012. Migraine: A disorder of brain excitatory–inhibitory balance? Trends Neurosci. 35, 507–520.
Westenbroek, R.E., Sakurai, T., Elliott, E.M., Hell, J.W., Starr, T.V.B., Snutch, T.P., Catterall, W.A., 1995. Immunochemical identification and subcellular distribution of the α_{1A} subunits of brain calcium channels. J. Neurosci. 15, 6403–6418.
Xue, M., Rosenmund, C., 2009. The headache of a hyperactive calcium channel. Neuron 61, 653–654.
Zaitsev, A.V., Povysheva, N.V., Lewis, D.A., Krimer, L.S., 2007. P/Q-type, but not N-type, calcium channels mediate GABA release from fast-spiking interneurons to pyramidal cells. J Neurophysiol 97, 3567–3573.